

Review

A Brief Overview of Recent Progress in Porous Silica as Catalyst Supports

Preeti S. Shinde ¹, Pradnya S. Suryawanshi ¹, Kanchan K. Patil ¹, Vedika M. Belekar ¹, Sandeep A. Sankpal ², Sagar D. Delekar ² and Sushilkumar A. Jadhav ^{1,*} 

¹ School of Nanoscience and Technology, Shivaji University Kolhapur, Vidyanagar, Kolhapur, Maharashtra 416004, India; preetishinde114@gmail.com (P.S.S.); pradnyasuryawanshi0607@gmail.com (P.S.S.); kanchanpatil66891@gmail.com (K.K.P.); vedikab1899@gmail.com (V.M.B.)

² Department of Chemistry, Shivaji University Kolhapur, Vidyanagar, Kolhapur, Maharashtra 416004, India; sandeeporg1@gmail.com (S.A.S.); sddelekar7@gmail.com (S.D.D.)

* Correspondence: sushil.unige@gmail.com; Tel.: +91-0231-260-9000

Abstract: Porous silica particles have shown applications in various technological fields including their use as catalyst supports in heterogeneous catalysis. The mesoporous silica particles have ordered porosity, high surface area, and good chemical stability. These interesting structural or textural properties make porous silica an attractive material for use as catalyst supports in various heterogeneous catalysis reactions. The colloidal nature of the porous silica particles is highly useful in catalytic applications as it guarantees better mass transfer properties and uniform distribution of the various metal or metal oxide nanocatalysts in solution. The catalysts show high activity, low degree of metal leaching, and ease in recycling when supported or immobilized on porous silica-based materials. In this overview, we have pointed out the importance of porous silica as catalyst supports. A variety of chemical reactions catalyzed by different catalysts loaded or embedded in porous silica supports are studied. The latest reports from the literature about the use of porous silica-based materials as catalyst supports are listed and analyzed. The new and continued trends are discussed with examples.

Keywords: porous silica; catalyst; heterogeneous catalysis; catalyst support; stability



Citation: Shinde, P.S.; Suryawanshi, P.S.; Patil, K.K.; Belekar, V.M.; Sankpal, S.A.; Delekar, S.D.; Jadhav, S.A. A Brief Overview of Recent Progress in Porous Silica as Catalyst Supports. *J. Compos. Sci.* **2021**, *5*, 75. <https://doi.org/10.3390/jcs5030075>

Academic Editors: Francesco Tornabene and Salet Balula

Received: 7 February 2021
Accepted: 3 March 2021
Published: 6 March 2021

Publisher's Note: MDPI stays neutral with regard to jurisdictional claims in published maps and institutional affiliations.



Copyright: © 2021 by the authors. Licensee MDPI, Basel, Switzerland. This article is an open access article distributed under the terms and conditions of the Creative Commons Attribution (CC BY) license (<https://creativecommons.org/licenses/by/4.0/>).

1. Introduction

Porous silicas are chemically and thermally stable materials with uniform pore size, pore distribution, high surface area, and high adsorption capacity [1–3]. The size and shape of the porous silica particles as well as the structure of pores on them can be tuned by controlling synthetic parameters like temperature, reaction time, and the amount of silicates/silica source; adjusting the surfactant concentration; changing the calcination conditions; etc. [4,5]. The pore size and its uniformity contribute to the strength of porous silica material [6]. A huge number of reports appear in the literature on silica and porous silica materials and their applications [7–13]. This shows their versatility and use in various technological or industrial applications. In particular, mesoporous silica nanoparticles are useful in several fields of application, such as environmental, biomedical, energy, and as catalyst supports [14]. They are also used in drug delivery [15], vaccine development, biomass conversion, and as catalyst or catalyst supports [16]. Due to the ordered porosity and unique features, they also act as highly efficient nano adsorbents for the adsorption removal of various toxic pollutants [17,18]. These extended applications of porous silica particles are due to the ease of their functionalization of both the internal and external surfaces of their pores with various organic functional groups [19]. The porous silica particles can also be used as a strong support matrix in catalytic applications [20].

The first report about the synthesis of ordered mesoporous silica material was in early 1990 [21]. Recently, there are several modified and new synthetic techniques for

the synthesis of porous silica particles. The newly invented techniques provide some advantages over the old methods. They offer control over synthesis conditions during nucleation and growth process [22]. Due to this, it is possible to produce silica nanoparticles with pore diameters ranging from microporous (below 2 nm) and mesoporous (2–50 nm) to macroporous (above 50 nm) [23]. The most common types of silica materials in the mesoporous pore size range are Mobil Crystalline Materials-41 (MCM-41) [24]; Santa Barbara Amorphous (SBA-15) [25,26] with hexagonal pore structure; and other types such as Hiroshima Mesoporous Material (HMM-33), Technical Delft University (TUD-1), folded sheets mesoporous materials (FSM-16), SBA-16, MCM-48, SBA-11, SBA-12, SBA-16, KIT-5, etc. Table 1 enlists the most common types of porous silica particles with their characteristic features and properties. Figure 1 shows the structures of different types of mesoporous silica nanoparticles. Due to the excellent chemical stability and the possibility of incorporation of various nanomaterials (catalysts), porous silica materials have received increased attention as catalyst supports. Among the various types of mesoporous silica materials mentioned above, MCM-50, SBA-11, and SBA-12 are reported as excellent adsorbent and catalytic supports [27].

Table 1. List of different types of mesoporous silica nanoparticles (MSNs) and their characteristic properties [27].

MSN Family	MSN Type	Pore Symmetry	Pore Size (nm)	Pore Volume (cm ³ /g)
M41S	MCM-41	2D hexagonal	1.5–8	>1.0
	MCM-48	3D cubic	2–5	>1.0
	MCM-50	Lamellar	2–5	>1.0
SBA	SBA-11	3D cubic	2.1–3.6	0.68
	SBA-12	3D hexagonal	3.1	0.83
	SBA-15	2D hexagonal	6–0	1.17
	SBA-16	Cubic	5–15	0.91
KIT	KIT-5	Cubic	9.3	0.45
COK	COK-12	Hexagonal	5.8	0.45
FDU	FDU-12	3D Cubic	10–26	0.66

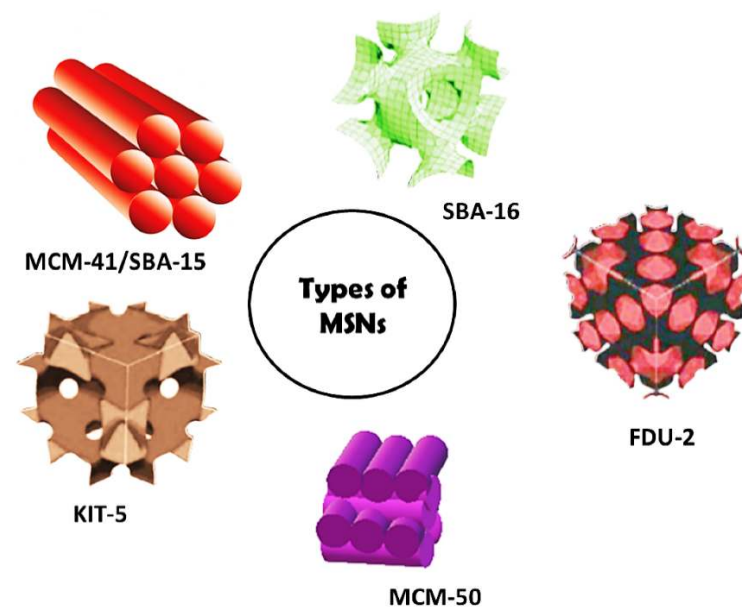


Figure 1. Different types of mesoporous silica nanoparticles. Reproduced with permission from the authors of [27].

The solid or porous silica materials are most commonly synthesized by sol-gel and hydrothermal processes. These methods include the use of reagents such as tetraethoxysilane (TEOS) as a silica source, cetyltrimethylammonium bromide (CTAB) as a templating agent, trimethyl benzene (TMB) as a modulator to tune the pore diameter, and alcohol as a solvent in combination with water [28,29]. The most established way to synthesize the catalyst-immobilized porous silica is using catalyst material as a base in a sol-gel process that will result in densely structured particles impregnated on or inside the highly branched silica network [30]. The composition and pore structure of the catalyst-immobilized porous silica materials can be studied with various characterization techniques such as infrared spectroscopy (IR), X-ray diffraction (XRD), thermogravimetric analysis (TGA), Brunauer-Emmett-Teller (BET), scanning electron microscopy (SEM), transmission electron microscopy (TEM), and nuclear magnetic resonance (NMR) [31,32]. These techniques can be used to conform the formation of siloxane network, porosity, formation, and incorporation of the catalyst particles in the silica matrix. Porous silicas are good catalyst supports because of their inertness, multi-functionalities, and stability in almost all solvents and high catalytic selectivity. The first report of using mesoporous silica in a polymer synthesis catalysis was reported by Aida's group in Japan, which opened a new route for advanced solid supported catalysis [33]. Their ability to catalyze (by virtue of the catalyst loaded) any reaction of alkylation, arylation, or vinylation of various alkenes in organic catalysis makes them an attractive material [34]. Their ability to readily separate from the product after reaction completion is another characteristic feature of porous silicas [35]. Porous silica-based materials have also been investigated as supports for enzymes such as cytochrome C (MW-12k) and showed that the immobilization of enzymes on inorganic material like porous silica is very useful in practical applications [36]. This is a classic example of the potential of porous silicas to improve the stability of biomolecules or an enzyme under extreme conditions. In this brief review, we have presented basic information about porous silica particles and highlighted their use as catalyst supports. The requirements of good catalyst supports are discussed, and the very latest reports from the literature about the use of porous silica-based materials as catalyst supports are enlisted with analysis.

MCM: Mobil Crystalline Materials; SBA: Santa Barbara Amorphous; KIT: Korea Advanced Institute of Science and Technology, COK: Centre for Research Chemistry and Catalysis Mobil Crystalline, FDU: Fairleigh Dickinson University.

2. Catalyst Support Properties and Requirements

Catalyst supports are important to support solid catalysts as they increase the efficiency of the supported metals or metal oxides by acting as a catalytically active center. The support can be chemically inert or it may interact with the active component (actual catalyst). Note that the interactions of the reactants in solid, liquid, or in gaseous forms with the support material must be non-destructive. The interactions of the support material with the active catalyst thereby affect the catalyst activity and selectivity. The support material may not contribute directly to the catalytic reaction process but may contribute indirectly by adsorbing the reactants near the embedded catalysts. The materials used as catalyst supports must show chemical stability, high surface area, as well as capability of dispersing metal or metal oxide particles highly over their surface. This is very important when expensive metals, such as gold, silver, platinum, ruthenium, palladium, etc., are used as the catalysts. Nanoparticles of noble metals are prepared to obtain the catalyst with high surface area and the supports must expose the right sides or maximum surface of the nanomaterials for the chemical reaction to occur. Supports give the catalyst its physical form, texture, mechanical resistance, and certain activity particularly for bifunctional catalysts. The surface chemical (functional groups) and physical properties of surfaces affect the performance of the supported metals. By keeping in mind these requirements, various oxides and carbon compounds are being used as catalyst support materials. Among all materials, silica (SiO₂) acts as an excellent catalyst support material due to its outstanding chemical and physical properties. The porosity plays an important role in increasing the

efficiency of catalyst supports. The shape as well as the size of pores of the support have an important effect on the activity and stability of embedded catalysts. Metal nanoparticles supported on porous silica-based supports exhibit higher catalytic activity arising from the higher accessibility of the active sites. A variety of porous silica particles are available as catalyst supports. Table 2 lists the main types of porous silica materials used as catalyst supports and their characteristic properties. The chemical inertness and high stability make these materials ideal catalyst supports. Figure 2 shows a representative example of how nickel nanoparticles are loaded or trapped inside different types of mesoporous silica-based catalyst supports. The different arrangements of the embedded catalyst inside the porous silica are clearly visible.

Table 2. Comparison of the properties of various porous silica particles.

Full Name	Santa Barbara Amorphous Type 15	Santa Barbara Amorphous Type 16	Mobil Composition of Matter No. 41	Mobil Composition of Matter No. 48	Hexagonal Mesoporous Silica
Short name	SBA-15	SBA-16	MCM-41	MCM-48	HMS
Structure directing agent	Pluronic 123 (non-ionic)	Pluronic F127 (non-ionic)	CTAB (cationic)	CTAB (cationic)	Amines (non-ionic)
pH at synthesis	Acidic (pH ~ 1)	Acidic (pH ~ 1)	Basic (pH ~ 11–13)	Basic (pH ~ 11–13)	Basic (pH ~ 9)
Features	Hexagonal pores, 2D array, <i>p6mm</i> symmetry, channels interconnected by small micropores	3D cubic arrangement connected by spherical cavities, <i>Im3m</i> space symmetry	1D mesopores, <i>p6mm</i> hexagonal, absence of interconnected pores	<i>la3d</i> 3D cubic continuous pore arrangement	Sponge-like particles, warm-hole mesostructured framework
Pore diameter	Uniform and larger pore diameter (4–30 nm) facilitating easy diffusion	Similar pore diameter values but nonuniform mesopores	Smaller pore diameter (1.5–10 nm) hindering the diffusion of substrates	Smaller pore diameter (2–3 nm) hindering the diffusion of substrates	Smaller pore diameter than SBA-15 (2–10)
Range of surface area	Higher surface area (~1000 m ² /g), high surface area to volume ratio	Comparable surface area values to SBA-15	Lower surface area (~800 m ² /g)	Higher surface area (~1100 m ² /g)	Surface area (800–1000 m ² /g)
Stability	Thick walls (up to 9 nm) and hence more thermally stable	Thick walls comparable to SBA-15	Thin walls (0.5 nm) and thus poor hydrothermal stability	Thin walls and hence comparatively less thermally stable	Less ordered structure but comparable stability

There are some important points that need to be considered both during the post-synthesis loading of the catalysts and in situ synthesis and loading of the catalyst particles on the porous silica-based supports. During in situ synthesis (generation), the catalyst particles get embedded inside the porous catalyst supports and may improve the overall mechanical stability of the porous support matrix. Instead, the post-synthesis loading of the catalyst particles inside the porous supports may pose some problems such as pore blocking (as seen in some images in Figure 2). Therefore, the size of the catalyst particles during post-synthesis immobilization must be smaller than the pore size. The blocking of the pores will prevent the reactant in various states to enter the pores and the overall conversion will be low. The covalent immobilization of catalyst particles during the post-synthesis catalyst loading is also essential. The catalyst particles can be held by strong bonds between the support and the surface of the catalyst. However, there is high likelihood of compromising the catalyst surface for surface modification and subsequent covalent immobilization reactions, which will affect the efficiency of the catalyst. The

percentage of loading (with respect to the weight of the porous catalyst support) of the catalyst can greatly affect the stability of the support matrix as well as the catalytic efficiency. An optimum loading of the catalyst is necessary for efficient performance of the catalyst in the reaction to be catalyzed. The shape of the pores available or created on the porous matrix/particles also play an important role in determining the efficiency of the material. If the shape of the catalyst particles and the pores is the same, then there is great possibility of proper filling of the pores by catalyst particles. The post-synthesis covalent immobilization of the catalyst and in situ synthesis and deposition of the catalyst on porous silica-based supports guarantee high stability of the material.

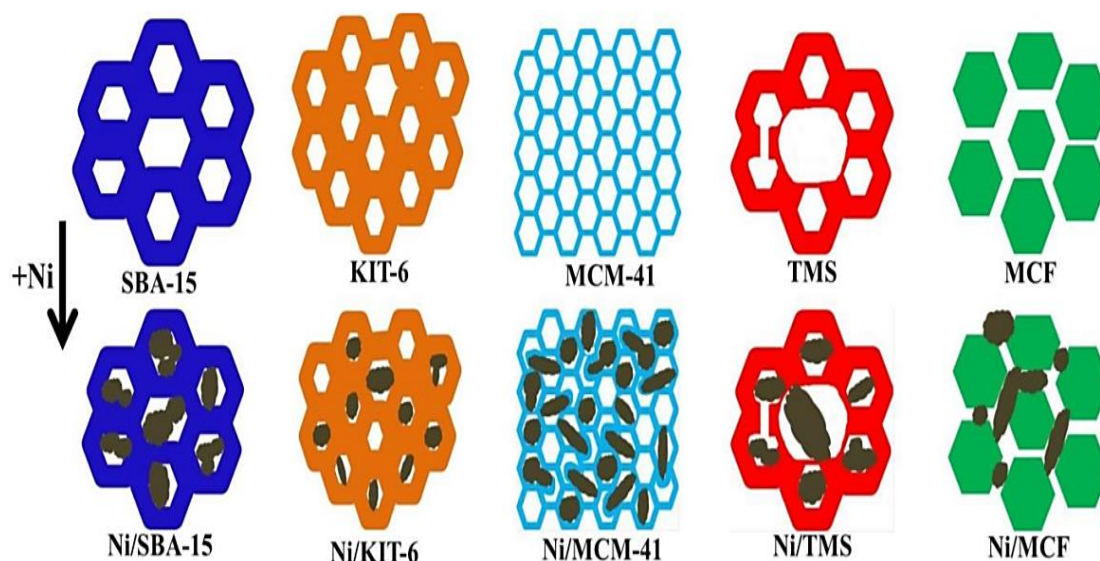


Figure 2. Schematic of the confinement effect on the Ni nanoparticles trapped inside the channels of supports. Reproduced with permission from the authors of [37].

3. Types of Reactions

The versatility and stability of the porous silica-based catalyst supports are evidenced by a variety of chemical reactions catalyzed by different catalysts supported on them. The porous silica-based catalyst supports are used in the reactions such as aerobic oxidation of alcohols (1-phenylethanol and benzyl alcohol) [38]; oxidation of methane to methanol [39,40], propene [41], benzene, benzyl alcohol [42], and toluene [43]; oxidative removal of 4,6-dimethyldibenzothiophene [44]; photooxidation of CO [45]; CO oxidation at low temperature [46–48]; organic oxidation of 1,2-dichloropropane [49,50]; photodegradation of methylene blue [51]; CO₂ adsorption [52–54]; hydrodeoxygenation of anisole [55]; esterification to produce biofuels [56,57]; biodiesel production from palm acid distillate [58]; biofuel upgrade (hydrocracking of camelina FAMES) [59]; model transesterification reaction (ethyl acetate + methanol = methyl acetate) [60]; dehydration of glycerol [61]; hydrodesulfurization [62]; decomposition of N₂O [63] and formic acid (HCOOH \leftrightarrow H₂ + CO₂) [64]; cycloisomerization of alkyne acids to alkylidene lactones [65]; coupling reactions (clean synthesis) [4,66,67]; carbon-carbon bond forming reactions [68]; removal of exhaust gas pollutant [69]; waste water treatment [70]; polymerization of olefins [71–73]; biodegradable polymer synthesis [74]; hydrocracking of pyrolyzed α -cellulose [75]; dehydration transfer hydrogenation [76]; selective hydrogenation of butadiene [77]; hydrogenation of methanol [78]; p-nitrophenol to p-aminophenol [79]; dehydrogenation [80–84]; CO₂ to methanol (CH₃OH) [85]; epoxidation of styrene [86–88]; cyanosilylation [33]; reduction of N₂ to ammonia [89]; bromate [90]; photocatalytic water oxidation [91]; photocatalytic degradation and removal of Cr(VI) and methylene blue [92]; photocatalytic hydrogen evolution from water [93]; catalytic transfer hydrogenation for the synthesis of γ -valerolactone [94,95];

Friedel-Craft alkylation reaction of aromatic compounds [96]; addition of carbon heteroatom bond formation [97]; and soot combustion [98].

A classic example of use of porous silica as catalyst supports is shown in Figure 3. It shows highly monodispersed palladium nanoparticles immobilized in three-dimensional dendritic mesoporous silica used as catalyst in Suzuki-Miyaura C-C cross-coupling. Instead, Figure 4 shows AuPt alloy yolk@shell hollow nanoparticles and their incorporation into hollow interiors of a mesoporous silica microspheres based on a rapid aerosol process. The AuPt@SiO₂ spheres showed excellent catalytic performance in the epoxidation of styrene with conversion and selectivity of 85% and 87%, respectively. Note that the various reactions mentioned above include different reactions conditions and states of the reactants, solvents, and other chemicals, and the silica-based catalyst support withstands all those conditions, proving its chemical stability, which is the prime requirement of the catalyst support as mentioned above.

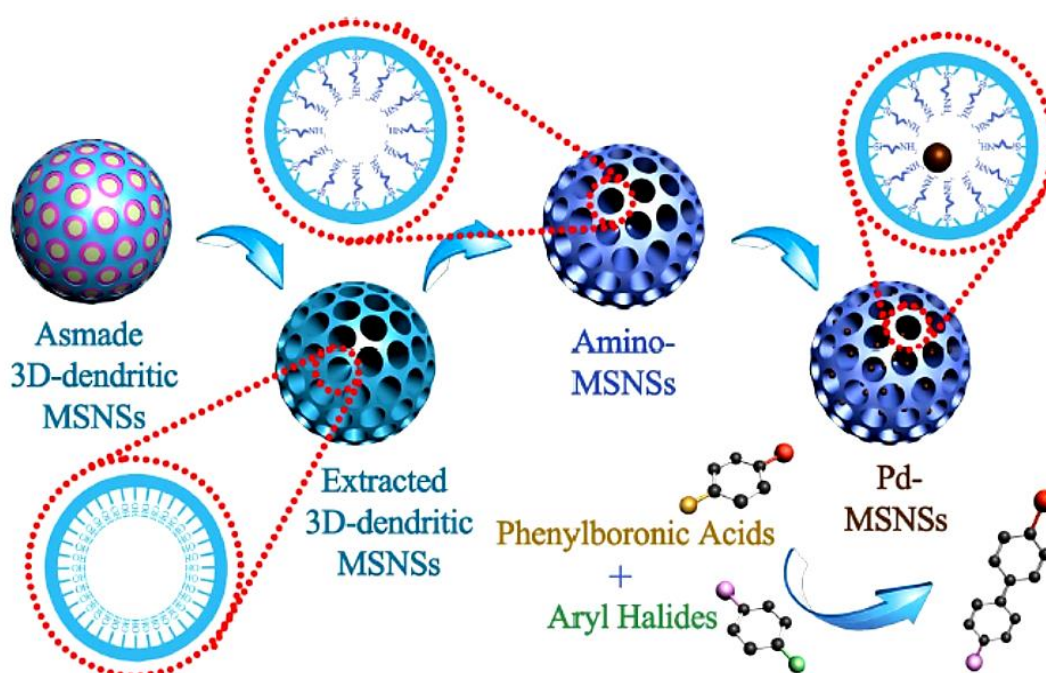


Figure 3. Synthesis and catalytic process of highly monodispersed palladium nanoparticles immobilized in three-dimensional dendritic mesoporous silica. Reproduced with permission from in [99].

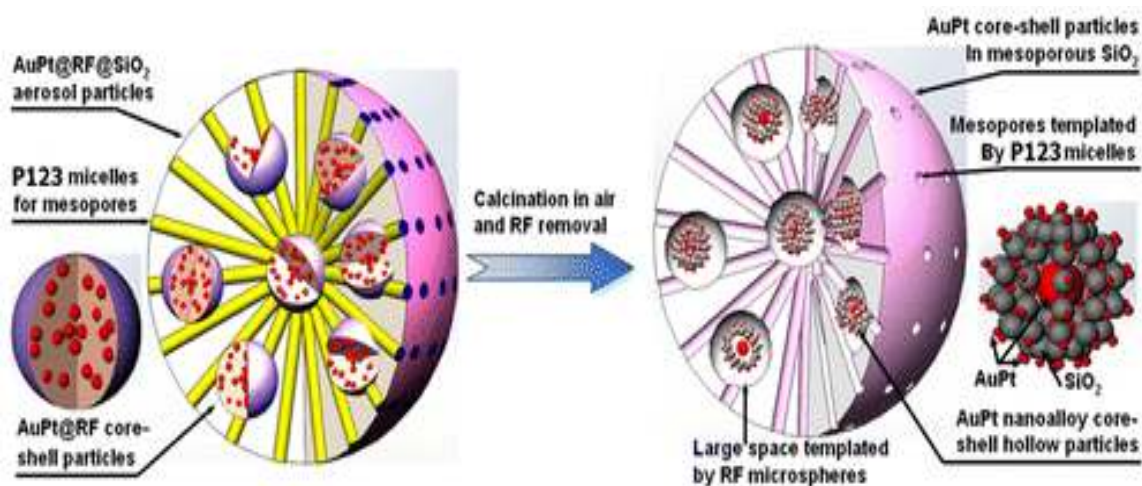


Figure 4. AuPt nanoalloy yolk@shell hollow particles in ordered mesoporous silica microspheres. Reproduced with permission from the authors of [100].

4. Recent Reports, Analysis and Trends

The very latest reports from the literature about porous silica-based catalyst supports are enlisted in Table 3 with the name of the catalyst material and reactions catalyzed. Observation of the entries in Table 3 reveals some trends about the use of porous silica-based materials as catalyst supports. Due to its simplicity and efficiency to produce monodispersed porous silica particles, the sol-gel technique remains the most common synthesis technique to obtain the porous supports. The trend of in situ synthesis and loading of the catalysts in the same synthesis conditions is also observed. The soft (easily degradable) template approach is the preferred technique to generate the porosity, and it is observed in most of the reports. Instead, a variety of different catalysts, such as noble metal nanoparticles, bimetallic nanoparticles, composite nanoparticles, alloys, noble metal, composite material nanocrystals, etc., are embedded in the porous silica-based supports. The pore sizes were tuned as per the sizes of various catalysts embedded in the materials. A variety of new reactions are added to the previously reported reactions as pointed out above. Most of the latest works also cover the studies of recyclability of the catalysts immobilized on silica-based catalyst supports, this proves the good hydrothermal or solvothermal (considering the fact that aqueous as well various solvents are used in the various reactions carried out) stability of the porous silica network. This is important from a technology and cost point of view. All the reports suggest the improved catalytic performance of the catalysts in various chemical reactions upon their immobilization on the porous silica-based catalyst supports. In addition to mere catalyst supports, some of the very interesting works report the chemical reactions catalyzed by porous silicas or by functional (that is organic functional group bearing) porous silica nanoparticles.

Table 3. Summary of the latest reports from the literature about the use of porous silica-based catalyst supports.

Sr. No.	Material	Type of Synthesis	Catalyst	Chemical Reaction	Ref.
1.	Core-shell structured magnetic silica.	Sol-gel	Bronsted acid	Transesterification of soybean oils, low-quality oils to biodiesel	[101]
2.	Chondroitinase ABC (I) on red porous silicon nanoparticles	Electrochemical etching	chondroitinase	Biological enzyme catalysis reaction	[102]
3.	Mesoporous-silica-supported metal nanocatalysts	Sol-gel	Metal nanocatalyst (Ag, Pd, amines)	Dehydrogenation of formic acid for Hydrogen generation ($\text{HCOOH} \rightarrow \text{H}_2 + \text{CO}_2$)	[103]
4.	Mesoporous silica (SBA-15, MCM-41)	Sol-gel	Palladium and platinum nanoparticles	Organic synthesis alcohols, carboxylic acids, and esters	[104]
5.	Mesoporous silica spheres and nanocapsules	Soft and hard dual template	Sulfonic acid	Biomass valorization catalysis, conversion of cellobiose into glucose	[105]
6.	Silica nanoshell ($\text{Pd}/\text{Fe}_3\text{O}_4@h\text{-SiO}_2$)	Sol-gel	Pd nanocrystals	Biorthogonal Organic Synthesis, carbocyclization reactions, converting a range of non-fluorescent substrates to fluorescent products	[106]
7.	Mesoporous fumed silica	Sol-gel	Palladium, Cobalt, Nickel, and Copper	Suzuki cross-coupling (SCC) reactions (C-C bond forming reaction) Cross-coupling reaction between bromobenzene with benzenboronic acid give biphenyl	[107]

Table 3. Cont.

Sr. No.	Material	Type of Synthesis	Catalyst	Chemical Reaction	Ref.
8.	Mesoporous MoO ₃ /SiO ₂ nanosphere networks	Self-assembly	MoO ₃	oxidative desulfurization of Dibenzothiophene (DBT)	[108]
9.	Silica	Sol-gel	IrO ₂	Photodegradation of methylene blue	[109]
10.	Dendrimer-like Porous Silica Nanoparticles (DPSNs)	Template-mediated self-assembly	Cu-BTC MOFs	Catalytic aerobic epoxidation of olefins, cyclooctene to cyclooctane oxide	[110]
11.	Mesoporous Silica (Fe@silica)	Sol-gel and Hydrothermal	Iron	Oxidation	[82]
12.	Silica (CuO@SiO ₂)	Sol-gel	Cu nanoparticles (NPs)	Cu-catalyzed organic transformations, C-C bond formation, reduction of organic dye	[111]
13.	Mesoporous silica matrix (MMS)	Direct growth technique	Hongkong University of Science and Technology (HKUST-1) (Cu ₃ (BTC) ₂ , BTC $\frac{1}{4}$ benzene-1,3,5-tricarboxylate) nanoparticles	Condensation reaction, Friedlander reaction between 2-amino-5-chlorobenzophenone and acetylacetone and Henry reaction nitroaldol condensation between nitromethane and 4-nitrobenzaldehyde	[112]
14.	Functionalized mesoporous SBA-15, SBA-16, MCM-41, MCM-48	Sol-gel	Metal nanoparticles (Ti, V, Cr, and Mo)	Catalytic transformation, Dry Reforming of Methane (DRM) reaction as CH ₄ + CO ₂ → 2H ₂ + 2CO	[33]
15.	Porous SiO ₂ (Pt@HS-SiO ₂ PL)	So-gel	Platinum Nanoparticles	Hydrogenation of alkenes (decene to decane) and nitroarenes to amino phenol	[113]
16.	Silica (SiO ₂) powder	Sol-gel	Diethylenetriamine	Knoevenagel reaction (carbon-carbon (C-C) coupling).	[114]
17.	Biosilica Microparticles	Diatom (<i>Thalassiosira pseudonana</i>)	Horseradish peroxidase (HRP), glucose oxidase, Gold nanoparticles	Biological enzyme catalysis reaction of <i>T. pseudonana</i> , Oxidation of glucose.	[115]
18.	Folic acid-functionalized dendritic fibrous nano-silica (FA-KCC-1-NH ₂) (FA = Folic acid, KCC-I = fibrous nano silica)	Hydrothermal	KCC-1-NH-FA nanoparticles	Amidation of carboxylic acids with amines	[116]
19.	Monodisperse mesoporous silica microspheres (M-MSMs)	Sol-gel	Au Nanoparticles	Reduction of 4-nitrophenol (4-NP) to 4-amino phenol	[117]
20.	CaSiO ₃ -SiO ₂ powder	Co-precipitation method	CaSiO ₃ (Na ₂ O·nSiO ₂)	Decomposition of isopropyl alcohol, dehydrogenation of the alcohol producing acetone	[118]
21.	ReO ₃ /SiO ₂ , silica matrix	Sol-gel	ReO ₃ nanoparticles	Photodegradation of Blue Methylene	[119]

Table 3. Cont.

Sr. No.	Material	Type of Synthesis	Catalyst	Chemical Reaction	Ref.
22.	Porous silicon dioxide (SiO ₂) and carboxyl-functionalized carbon nanotube (PtIrNi/SiO ₂ -CNT-COOH)	Sol-gel	PtIrNi alloy nanoparticles	Electrochemical Ammonia Oxidation reaction (AOR)	[120]
23.	Expanded mesoporous silica (EMSN)-encapsulated Pt nanoclusters.	Sol-gel	Pt nanoclusters	Artificial enzymes for tracking hydrogen peroxide secretion from live cells	[121]
24.	Microporous silica microcapsules	Gas-in-water-in oil emulsions (g/w/o)	Microporous silica microcapsules	Ostwald ripening, generation of gas-in-water-in-oil emulsions	[122]
25.	Pt-loaded ZSM-22/MCM-4 (Pt-MES)	Sol-gel	Bronsted acid, Pt nanoparticles	N-alkane isomerization for refinery process by converting the petroleum into the gasoline with high quality and the diesel	[90]
26.	Organo-amine-functionalized castor oil templated mesoporous silicas	Valorization of rice husk	Amine groups	Biodiesel synthesis, transesterification of model C4-C12 triglycerides (TAG) to fatty acid methyl esters	[123]
27.	TEMPO-functionalized mesoporous silica particles, MCM-41 and SBA-	Co-condensation	(2,2,6,6-tetramethylpiperidin-1-yl) oxyl (TEMPO)	Heterogeneous oxidation (oxidation of alcohols to aldehydes), Knoevenagel condensation (C-C bond formation)	[124]
28.	Silica-encapsulated core-shell Co@SiO ₂	Hydrothermal	Cobalt	Fischer-Tropsch synthesis (FTS)	[125]
29.	Porous silica	Sol-gel	Gold nanoparticles	Biomedical, catalytic, and optical properties	[14]
30.	Palladium Nanocatalysts Encapsulated on Porous Silica @ Magnetic Carbon-Coated Cobalt Nanoparticles	Sol-gel	Palladium nanoparticles	Sustainable hydrogenation of nitroarenes to aniline, alkenes and alkynes	[126]
31.	SBA-15-based composites (X@SBA-15)	Impregnation and hydrothermal methods	Transition metals/metal oxides and nanocarbons	Water decontamination by advanced oxidation processes	[25]
32.	Mesoporous silica	Sol-gel	Ni-Co bimetallic hydroxide particles	Urea oxidation reaction	[127]
33.	Porous silica nanotubes loaded Au nanoparticles (SiO ₂ @Au@SiO ₂ NTs)	Sol-gel	Gold nanoparticles	Catalytic reduction of 4-Nitrophenol to 4-amino phenol	[128]
34.	Self-propelled mesoporous silica nanorods (MSNRs)	Sol-gel	Iron oxide (Fe ₂ O ₃) nanoparticles	Catalytic decomposition of hydrogen peroxide by a sputtered Pt layer	[129]
35.	Porous silica	Self-assembly	Metal and alloy nanoparticles (Au, Ag, Pd, Ag/Pd)	Biom mineralization, reduction of 4-nitrophenol to 4-amino phenol	[130]

Table 3. Cont.

Sr. No.	Material	Type of Synthesis	Catalyst	Chemical Reaction	Ref.
36.	A novel and yolk/shell nanoreactor catalyst (H-Fe ₃ O ₄ @h-CuO@m-SiO ₂)	Hydrothermal	CuO-nanoparticles	A3 coupling reaction of alkynes, aldehydes, and amines	[131]
37.	Micron-sized, spherical SiO ₂	Mechanochemical	Spherical silica	Polyolefin catalyst production	[132]
38.	Ni@SiO ₂ core-shell nanocatalysts	Sol-gel	Ni particles	Catalytic oxidation of CH ₄ to CO ₂	[133]
39.	Hollow SiO ₂ spheres	Template synthesis	Au nanoparticles	Catalytic Microreactors, reduction of 4-nitrophenol to 4-aminophenol	[134]
40.	Monolacunary Keggin-type [PW11O39] 7-(PW11) heteropolyanion SBA-15 (PW11@TMA-SBA-15)	Sol-gel	N-trimethylammonium (TMA)	Oxidative desulfurization of organosilica composite	[135]
41.	Porous silica	Sol-gel	Ni nanocatalyst	Thermal gasification of waste biomass	[136]
42.	Macroporous SiO ₂	Sol-gel	Ag ₂ O, Na ₂ O or K ₂ O	Soot combustion reactions, gas-solid-solid reactions	[137]
43.	Aminopropyl functionalized mesocellular foam silica (MCF)	Sol-gel	Penicillin acylase	6-aminopenicillanic acid production, biocatalytic transformation	[138]
44.	TiO ₂ /SiO ₂ /C nanofiber mat, SiO ₂ nanoparticles	Calcination	TiO ₂ /SiO ₂ /C	Photocatalytic degradation of organic pollutants (rhodamine B and 4-nitrophenol) in water	[139]
45.	Alumina-coated silica nanoparticles (AlO-SiO NPs)	Sol-gel	Alumina	Surface reactions	[140]
46.	mesoporous g-C ₃ N ₄ /SiO ₂ material	Sol-gel	Carbon nitride (g-C ₃ N ₄)	Photodegradation of rhodamine B (RhB) under visible light	[141]
47.	Mesoporous silica material KIT-6	Template synthesis	Transition metals	Electrocatalytic hydrogen evolution reaction	[142]
48.	Pd/SiO ₂ and Fe/SiO ₂	Sol-gel	Metallic (Pd catalysts) or metallic oxide (Fe catalysts) nanoparticles	Pd/SiO ₂ Hydrodechlorination of 2,4,6-trichlorophenol (TCP) in water, Fe/SiO ₂ materials degrade phenol	[143]
49.	Bimodal porous silica	Sol-gel	NiO	Phenol to cyclohexanol	[144]
50.	Mesoporous silica materials (SBA-15 and MCM-41)	Sol-gel	Phosphonic and phosphoric acid esters	Asymmetric aldol reaction (C-C bond formation)	[145]
51.	Mesoporous silica (SBA-15)	Sol-gel	Laccase	Enzyme aggregate (E-CLEA) potential in phenol removal	[146]
52.	Novel hollow-Co ₃ O ₄ @Co ₃ O ₄ @SiO ₂ multi-yolk-double-shell nanoreactors	Sol-gel	Metals (Pd, Pt, Ru, Rh, and Au) and metal oxides.	CO Oxidation	[147]

Table 3. Cont.

Sr. No.	Material	Type of Synthesis	Catalyst	Chemical Reaction	Ref.
53.	Ordered mesoporous silicas (MCM-41)	Sol-gel	Aluminum	Hydro isomerization and Friedel-Crafts alkylation of benzene with benzyl alcohol	[148]
54.	Colloidal mesoporous silica nanoparticles (LP-MSNs)	Co-condensation	Alkyne-functionalized	Colorimetric reaction of guaiacol (2-methoxyphenol), hydrolysis of 4-nitrophenyl acetate (NPA) by LP-MSN-CA	[149]

5. Conclusions

This brief overview pointed out the importance of porous silica as catalyst supports. A huge number of reports in the literature on this topic prove the versatility and efficiency of porous silica as catalyst supports. A careful observation of the latest reports showed that some previous trends about the synthesis of porous silica supports and in situ generation and immobilization of the catalysts are continued. A variety of new, bimetallic, composite and functional nanocatalysts are embedded or immobilized on the porous silica nano and microparticles to efficiently catalyze various reactions. The research in this field will proceed in future along following main directions.

Development of functional silica-based porous particles embedded with various catalyst nanoparticles where synergic effects of the various organic functional groups grafted on the supports and the catalyst will assist the chemical transformations.

Further development and optimization of single step or in situ (or minimum steps) methods for the functionalization of the silica-based porous supports as well as synthesis and immobilization of the catalysts.

Development of the large-scale production methods for already reported various composite nanoparticles (catalyst) embedded in porous silica particles.

Author Contributions: Conceptualization, S.A.J.; writing—original draft preparation, P.S.S. (Preeti S. Shinde), P.S.S. (Pradnya S. Suryawanshi), K.K.P., V.M.B.; writing—review and editing, S.A.J., S.A.S., S.D.D.; supervision, S.A.J., S.A.S., S.D.D.; project administration, S.A.J. All authors have read and agreed to the published version of the manuscript.

Funding: This research received no external funding.

Conflicts of Interest: The authors declare no conflict of interest.

References

- Gawande, M.B.; Monga, Y.; Zboril, R.; Sharma, R. Silica-decorated magnetic nanocomposites for catalytic applications. *Coord. Chem. Rev.* **2015**, *288*, 118–143. [\[CrossRef\]](#)
- Lai, C.Y. Mesoporous Silica Nanomaterials Applications in Catalysis. *J. Thermodyn. Catal.* **2014**, *5*, 1–3. [\[CrossRef\]](#)
- Verma, P.; Kuwahara, Y.; Mori, K.; Raja, R.; Yamashita, H. Functionalized mesoporous SBA-15 silica: Recent trends and catalytic applications. *Nanoscale* **2020**, *12*, 11333–11363. [\[CrossRef\]](#)
- Polshettiwar, V.; Len, C.; Fihri, A. Silica-supported palladium: Sustainable catalysts for cross-coupling reactions. *Co-ord. Chem. Rev.* **2009**, *253*, 2599–2626. [\[CrossRef\]](#)
- Sun, M.-H.; Huang, S.-Z.; Chen, L.-H.; Li, Y.; Yang, X.-Y.; Yuan, Z.-Y.; Su, B.-L. Applications of hierarchically structured porous materials from energy storage and conversion, catalysis, photocatalysis, adsorption, separation, and sensing to biomedicine. *Chem. Soc. Rev.* **2016**, *45*, 3479–3563. [\[CrossRef\]](#) [\[PubMed\]](#)
- Wang, J.; Liu, C.; Qi, J.; Li, J.; Sun, X.; Shen, J.; Han, W.; Wang, L. Enhanced heterogeneous Fenton-like systems based on highly dispersed FeO-Fe₂O₃ nanoparticles embedded ordered mesoporous carbon composite catalyst. *Environ. Pollut.* **2018**, *243*, 1068–1077. [\[CrossRef\]](#) [\[PubMed\]](#)
- Jadhav, S.A. Incredible pace of research on mesoporous silica nanoparticles. *Inorg. Chem. Front.* **2014**, *1*, 735–739. [\[CrossRef\]](#)
- Sharma, N.; Ojha, H.; Bharadwaj, A.; Pathak, D.P.; Sharma, R.K. Preparation and catalytic applications of nanomaterials: A review. *RSC Adv.* **2015**, *5*, 53381–53403. [\[CrossRef\]](#)
- Kaur, M.; Sharma, S.; Bedi, P.M. Silica supported Brønsted acids as catalyst in organic transformations: A comprehensive review. *Chin. J. Catal.* **2015**, *36*, 520–549. [\[CrossRef\]](#)

10. Vincent, A.; Babu, S.; Brinley, E.; Karakoti, A.; Deshpande, A.S.; Seal, S. Role of Catalyst on Refractive Index Tunability of Porous Silica Antireflective Coatings by Sol–Gel Technique. *J. Phys. Chem. C* **2007**, *111*, 8291–8298. [[CrossRef](#)]
11. Cheraghian, G. Application of nano-fumed silica in heavy oil recovery. *Pet. Sci. Technol.* **2016**, *34*, 12–18. [[CrossRef](#)]
12. Jadhav, S.A.; Garud, H.B.; Patil, A.H.; Patil, G.D.; Patil, C.R.; Dongale, T.D.; Patil, P.S. Recent advancements in silica nanoparticles based technologies for removal of dyes from water. *Colloids Interf. Sci. Commun.* **2019**, *30*, 100181. [[CrossRef](#)]
13. Cheraghian, G.; Hemmati, M.; Bazgir, S. Application of TiO₂ and fumed silica nanoparticles and improve the performance of drilling fluids. *Electron. Photonic Plasmonic Phononic Magn. Prop. Nanomater.* **2014**, *270*, 266–270.
14. Kamiński, M.; Jurkiewicz, K.; Burian, A.; Bródka, A. The structure of gold nanoparticles: Molecular dynamics modeling and its verification by X-ray diffraction. *J. Appl. Crystallogr.* **2020**, *53*, 1–8. [[CrossRef](#)]
15. Jadhav, S.A.; Scalarone, D.; Brunella, V.; Berlier, G. Poly(NIPAM-co-MPS)-grafted multimodal porous silica nanoparticles as reverse thermoresponsive drug delivery system. *Asian J. Pharm. Sci.* **2017**, *12*, 279. [[CrossRef](#)] [[PubMed](#)]
16. Liang, J.; Liang, Z.; Zou, R.; Zhao, Y. Heterogeneous Catalysis in Zeolites, Mesoporous Silica, and Metal–Organic Frameworks. *Adv. Mater.* **2017**, *29*, 1–21. [[CrossRef](#)]
17. Barakan, S.; Aghazadeh, V. Structural modification of nano bentonite by aluminum, iron pillarization and 3D growth of silica mesoporous framework for arsenic removal from gold mine wastewater. *J. Hazard. Mater.* **2019**, *378*, 120779. [[CrossRef](#)]
18. Nayab, S.; Baig, H.; Ghaffar, A.; Tuncel, E.; Oluz, Z.; Duran, H.; Yameen, B. Silica based inorganic–organic hybrid materials for the adsorptive removal of chromium. *RSC Adv.* **2018**, *8*, 23963–23972. [[CrossRef](#)]
19. Kim, S.-H.; Shin, C.-K.; Ahn, C.-H.; Kim, G.-J. Syntheses and application of silica monolith with bimodal meso/macroscopic pore structure. *J. Porous Mater.* **2006**, *13*, 201–205. [[CrossRef](#)]
20. Bourlinos, A.B.; Simopoulos, A.; Boukos, A.N.; Petridis, D. Magnetic Modification of the External Surfaces in the MCM-41 Porous Silica: Synthesis, Characterization, and Functionalization. *J. Phys. Chem. B* **2001**, *105*, 7432–7437. [[CrossRef](#)]
21. Sen, T.; Tiddy, G.J.T.; Casci, J.L.; Anderson, M.W. Synthesis and Characterization of Hierarchically Ordered Porous Silica Materials. *Chem. Mater.* **2004**, *16*, 2044–2054. [[CrossRef](#)]
22. Giraldo, L.F.; López, B.L.; Pérez, L.; Urrego, S.; Sierra, L.; Mesa, M. Mesoporous Silica Applications. *Macromol. Symp.* **2007**, *258*, 129–141. [[CrossRef](#)]
23. Gupta, R.; Gupta, S.K.; Pathak, D.D. Selective adsorption of toxic heavy metal ions using guanine-functionalized mesoporous silica [SBA-16-g] from aqueous solution. *Microporous Mesoporous Mater.* **2019**, *288*, 109577. [[CrossRef](#)]
24. Wu, S.-H.; Mou, C.-Y.; Lin, H.-P. Synthesis of mesoporous silica nanoparticles. *Chem. Soc. Rev.* **2013**, *42*, 3862–3875. [[CrossRef](#)] [[PubMed](#)]
25. Yuanab, S.; Wanga, M.; Liub, J.; Guoc, B. Recent advances of SBA-15-based composites as the heterogeneous catalysts in water decontamination: A mini-review. *J. Environ. Manag.* **2020**, *254*, 109787. [[CrossRef](#)]
26. El-Nahhal, I.M.; Chehimi, M.; Selmane, M. Synthesis and Structural Characterization of G-SBA-IDA, G-SBA-EDTA and G-SBA-DTPA Modified Mesoporous SBA-15 Silica and Their Application for Removal of Toxic Metal Ions Pollutants. *Silicon* **2018**, *10*, 981–993. [[CrossRef](#)]
27. Narayan, R.; Nayak, U.Y.; Raichur, A.M.; Garg, S. Mesoporous Silica Nanoparticles: A Comprehensive Review on Synthesis and Recent Advances. *Pharmaceutics* **2018**, *10*, 118. [[CrossRef](#)] [[PubMed](#)]
28. Synthesis and Testing of Functional Mesoporous Silica Nanoparticles for Removal of Cr(VI) Ions From Water. *Biointerface Res. Appl. Chem.* **2020**, *11*, 8599–8607. [[CrossRef](#)]
29. Jadhav, S.A.; Patil, V.S.; Shinde, P.S.; Thoravat, S.S.; Patil, P.S. A short review on recent progress in mesoporous silicas for the removal of metal ions from water. *Chem. Pap.* **2020**, *74*, 4143–4157. [[CrossRef](#)]
30. Shimizu, W.; Hokka, J.; Sato, T.; Usami, H.; Murakami, Y. Microstructure Investigation on Micropore Formation in Microporous Silica Materials Prepared via a Catalytic Sol–Gel Process by Small Angle X-Ray Scattering. *J. Phys. Chem. B* **2011**, *115*, 9369–9378. [[CrossRef](#)]
31. Kumar, S.; Malik, M.; Purohit, R. *Synthesis Methods of Mesoporous Silica Materials*; Elsevier BV: Amsterdam, The Netherlands, 2017; Volume 4, pp. 350–357.
32. Jadhav, S.A.; Mileto, I.; Brunella, V.; Scalarone, D.; Berlier, G. Porous Silica Particles: Synthesis, Physicochemical Characterization and Evaluation of Suspension Stability. *Phys. Chem. Ind. J.* **2017**, 1–11.
33. Kageyama, K.; Tamazawa, J.-I.; Aida, T. Extrusion Polymerization: Catalyzed Synthesis of Crystalline Linear Polyethylene Nanofibers Within a Mesoporous Silica. *Science* **1999**, *285*, 2113–2115. [[CrossRef](#)] [[PubMed](#)]
34. Della Pina, C.; Falletta, E. Gold-catalyzed oxidation in organic synthesis: A promise kept. *Catal. Sci. Technol.* **2011**, *1*, 1564–1571. [[CrossRef](#)]
35. Sivasamy, A.; Cheah, K.Y.; Fornasiero, P.; Kemausuor, F.; Zinoviev, S.; Miertus, S. Catalytic Applications in the Production of Biodiesel from Vegetable Oils. *ChemSusChem* **2009**, *2*, 278–300. [[CrossRef](#)] [[PubMed](#)]
36. Takahashi, H.; Li, B.; Sasaki, T.; Miyazaki, C.; Kajino, T.; Inagaki, S. Catalytic Activity in Organic Solvents and Stability of Immobilized Enzymes Depend on the Pore Size and Surface Characteristics of Mesoporous Silica. *Chem. Mater.* **2000**, *12*, 3301–3305. [[CrossRef](#)]
37. Amin, M.H. Relationship between the Pore Structure of Mesoporous Silica Supports and the Activity of Nickel Nanocatalysts in the CO₂ Reforming of Methane. *Catalysts* **2020**, *10*, 51. [[CrossRef](#)]

38. Chu, X.; Wang, C.; Guo, L.; Chi, Y.; Gao, X.; Yang, X. Mesoporous Silica Supported Au Nanoparticles with Controlled Size as Efficient Heterogeneous Catalyst for Aerobic Oxidation of Alcohols. *J. Chem.* **2015**, *2015*, 1–7. [[CrossRef](#)]
39. Le, H.V.; Parishan, S.; Sagaltchik, A.; Ahi, H.; Trunschke, A.; Schomäcker, R.; Thomas, A. Stepwise Methane-to-Methanol Conversion on CuO/SBA-15. *Chem. A Eur. J.* **2018**, *24*, 12592–12599. [[CrossRef](#)]
40. Zhang, Q.; Li, Y.; An, D.; Wang, Y. Catalytic behavior and kinetic features of FeOx/SBA-15 catalyst for selective oxidation of methane by oxygen. *Appl. Catal. A Gen.* **2009**, *356*, 103–111. [[CrossRef](#)]
41. Fu, T.; Wang, Y.; Wernbacher, A.M.; Schlögl, R.; Trunschke, A. Single-Site Vanadyl Species Isolated within Molybdenum Oxide Monolayers in Propane Oxidation. *ACS Catal.* **2019**, *9*, 4875–4886. [[CrossRef](#)]
42. Nozaki, C.; Lugmair, C.G.; Bell, A.T.; Tilley, T.D. Synthesis, Characterization, and Catalytic Performance of Single-Site Iron(III) Centers on the Surface of SBA-15 Silica. *J. Am. Chem. Soc.* **2002**, *124*, 13194–13203. [[CrossRef](#)] [[PubMed](#)]
43. Qin, Y.; Qu, Z.; Dong, C.; Wang, Y.; Huang, N. Highly catalytic activity of Mn/SBA-15 catalysts for toluene combustion improved by adjusting the morphology of supports. *J. Environ. Sci.* **2019**, *76*, 208–216. [[CrossRef](#)] [[PubMed](#)]
44. Gonzalez, J.; Wang, J.A.; Chen, L.; Manriquez, M.E.; Dominguez, J.M. Structural Defects, Lewis Acidity, and Catalysis Properties of Mesostructured WO₃/SBA-15 Nanocatalysts. *J. Phys. Chem. C* **2017**, *121*, 23988–23999. [[CrossRef](#)]
45. Barroso-Martín, I.; Infantes-Molina, A.; Talon, A.; Storaro, L.; Rodríguez-Aguado, E.; Rodríguez-Castellón, E.; Moretti, E. CO Preferential Photo-Oxidation in Excess of Hydrogen in Dark and Simulated Solar Light Irradiation over AuCu-Based Catalysts on SBA-15 Mesoporous Silica-Titania. *Materials* **2018**, *11*, 1203. [[CrossRef](#)] [[PubMed](#)]
46. Moreno-Martell, A.; Pawelec, B.; Nava, R.; Mota, N.; Escamilla-Perea, L.; Navarro, R.M.; Fierro, J.L. CO Oxidation at 20 °C on Au Catalysts Supported on Mesoporous Silica: Effects of Support Structural Properties and Modifiers. *Materials* **2018**, *11*, 948. [[CrossRef](#)] [[PubMed](#)]
47. Al Soubaihi, R.M.; Saoud, K.M.; Ye, F.; Myint, M.T.Z.; Saeed, S.; Dutta, J. Synthesis of hierarchically porous silica aerogel supported Palladium catalyst for low-temperature CO oxidation under ignition/extinction conditions. *Microporous Mesoporous Mater.* **2020**, *292*, 109758. [[CrossRef](#)]
48. Al-Shehri, B.M.; Shkir, M.; Khder, A.S.; Kaushik, A.; Hamdy, M.S. Noble Metal Nanoparticles Incorporated Siliceous TUD-1 Mesoporous Nano-Catalyst for Low-Temperature Oxidation of Carbon Monoxide. *Nanomaterials* **2020**, *10*, 1067. [[CrossRef](#)]
49. Cheng, X.; Wang, D.; Liu, J.; Kang, X.; Yan, H.; Wu, A.; Gu, Y.; Tian, C.; Fu, H. Ultra-small Mo₂N on SBA-15 as a highly efficient promoter of low-loading Pd for catalytic hydrogenation. *Nanoscale* **2018**, *10*, 22348–22356. [[CrossRef](#)]
50. Finocchio, E.; Gonzalez-Prior, J.; Gutierrez-Ortiz, J.I.; Lopez-Fonseca, R.; Busca, G.; De Rivas, B. Surface Characterization of Mesoporous CoOx/SBA-15 Catalyst upon 1,2-Dichloropropane Oxidation. *Materials* **2018**, *11*, 912. [[CrossRef](#)]
51. Barroso-Martín, I.; Moretti, E.; Talon, A.; Storaro, L.; Rodríguez-Castellón, E.; Infantes-Molina, A. Au and AuCu Nanoparticles Supported on SBA-15 Ordered Mesoporous Titania-Silica as Catalysts for Methylene Blue Photodegradation. *Materials* **2018**, *11*, 890. [[CrossRef](#)]
52. Sánchez-Zambrano, K.S.; Duarte, L.L.; Maia, D.A.S.; Vilarrasa-García, E.; Bastos-Neto, M.; Rodríguez-Castellón, E.; De Azevedo, D.C.S. CO₂ Capture with Mesoporous Silicas Modified with Amines by Double Functionalization: Assessment of Adsorption/Desorption Cycles. *Materials* **2018**, *11*, 887. [[CrossRef](#)] [[PubMed](#)]
53. Kuwahara, Y.; Kang, D.-Y.; Copeland, J.R.; Brunelli, N.A.; Didas, S.A.; Bollini, P.; Sievers, C.; Kamegawa, T.; Yamashita, H.; Jones, C.W. Dramatic Enhancement of CO₂ Uptake by Poly(ethyleneimine) Using Zirconosilicate Supports. *J. Am. Chem. Soc.* **2012**, *134*, 10757–10760. [[CrossRef](#)] [[PubMed](#)]
54. Kuwahara, Y.; Kang, D.-Y.; Copeland, J.R.; Bollini, P.; Sievers, C.; Kamegawa, T.; Yamashita, H.; Jones, C.W. Enhanced CO₂ Adsorption over Polymeric Amines Supported on Heteroatom-Incorporated SBA-15 Silica: Impact of Heteroatom Type and Loading on Sorbent Structure and Adsorption Performance. *Chem. A Eur. J.* **2012**, *18*, 16649–16664. [[CrossRef](#)] [[PubMed](#)]
55. Jang, M.S.; Phan, T.N.; Chung, I.S.; Lee, I.-G.; Park, Y.-K.; Ko, C.H. Metallic nickel supported on mesoporous silica as catalyst for hydrodeoxygenation: Effect of pore size and structure. *Res. Chem. Intermed.* **2018**, *44*, 3723–3735. [[CrossRef](#)]
56. Kuwahara, Y.; Fujitani, T.; Yamashita, H. Esterification of levulinic acid with ethanol over sulfated mesoporous zirconosilicates: Influences of the preparation conditions on the structural properties and catalytic performances. *Catal. Today* **2014**, *237*, 18–28. [[CrossRef](#)]
57. Silva, Â.; Wilson, K.; Lee, A.F.; dos Santos, V.C.; Bacilla, A.C.C.; Mantovani, K.M.; Nakagaki, S. Nb₂O₅/SBA-15 catalyzed propanoic acid esterification. *Appl. Catal. B Environ.* **2017**, *205*, 498–504. [[CrossRef](#)]
58. Manga, J.; Ahmad, A.; Taba, P. Firdaus Synthesis and modification of mesoporous silica with sulfated titanium dioxide as a heterogeneous catalyst for biodiesel production from palm fatty acid distillate. *J. Phys. Conf. Ser.* **2019**, *1341*, 032014. [[CrossRef](#)]
59. Fei, L.; Reddy, H.K.; Hill, J.; Lin, Q.; Yuan, B.; Xu, Y.; Dailey, P.; Deng, S.; Luo, H. Preparation of Mesoporous Silica-Supported Palladium Catalysts for Biofuel Upgrade. *J. Nanotechnol.* **2012**, *2012*, 1–6. [[CrossRef](#)]
60. Zapelini, I.W.; Silva, L.L.; Cardoso, D. Effect of Hydrothermal Treatment on Structural and Catalytic Properties of [CTA]-MCM-41 Silica. *Materials* **2018**, *11*, 860. [[CrossRef](#)]
61. Cecilia, J.A.; García-Sancho, C.; Jiménez-Gómez, C.P.; Moreno-Tost, R.; Maireles-Torres, P. Porous Silicon-Based Catalysts for the Dehydration of Glycerol to High Value-Added Products. *Materials* **2018**, *11*, 1569. [[CrossRef](#)]
62. Huirache-Acuña, R.; Nava, R.; Peza-Ledesma, C.L.; Lara-Romero, J.; Alonso-Núñez, G.; Pawelec, B.; Rivera-Muñoz, E.M. SBA-15 Mesoporous Silica as Catalytic Support for Hydrodesulfurization Catalysts—Review. *Materials* **2013**, *6*, 4139–4167. [[CrossRef](#)]

63. Wei, X.; Yang, X.-F.; Wang, A.-Q.; Li, L.; Liu, X.-Y.; Zhang, T.; Mou, C.-Y.; Li, J. Bimetallic Au–Pd Alloy Catalysts for N₂O Decomposition: Effects of Surface Structures on Catalytic Activity. *J. Phys. Chem. C* **2012**, *116*, 6222–6232. [[CrossRef](#)]
64. Jin, M.-H.; Oh, D.-K.; Park, J.-H.; Lee, C.-B.; Lee, S.-W.; Park, J.-S.; Lee, K.-Y.; Lee, D.-W. Mesoporous Silica Supported Pd–MnOx Catalysts with Excellent Catalytic Activity in Room-Temperature Formic Acid Decomposition. *Sci. Rep.* **2016**, *6*, 33502. [[CrossRef](#)]
65. Verho, O.; Gao, F.; Johnston, E.V.; Wan, W.; Nagendiran, A.; Zheng, H.; Bäckvall, J.-E.; Zou, X. Mesoporous silica nanoparticles applied as a support for Pd and Au nanocatalysts in cycloisomerization reactions. *APL Mater.* **2014**, *2*, 113316. [[CrossRef](#)]
66. Macquarrie, D.J.; Gotov, B.; Toma, S. Silica-supported palladium-based catalysts for clean synthesis. *Platin. Met. Rev.* **2001**, *45*, 102–110.
67. Crudden, C.M.; Sateesh, M.; Lewis, R. Mercaptopropyl-Modified Mesoporous Silica: A Remarkable Support for the Preparation of a Reusable, Heterogeneous Palladium Catalyst for Coupling Reactions. *J. Am. Chem. Soc.* **2005**, *127*, 10045–10050. [[CrossRef](#)] [[PubMed](#)]
68. Erigoni, A.; Hernández-Soto, M.C.; Rey, F.; Segarra, C.; Díaz, U. Highly active hybrid mesoporous silica-supported base organocatalysts for C–C bond formation. *Catal. Today* **2020**, *345*, 227–236. [[CrossRef](#)]
69. Kobylinski, T.P.; Hammel, J.J.; Swift, H.E. Porous Silica Beads—A Catalyst Support for Removal of Exhaust Gas Pollutants. *Ind. Eng. Chem. Prod. Res. Dev.* **1975**, *14*, 147–150. [[CrossRef](#)]
70. Ding, Q.; Hu, X. Mesoporous Materials as Catalyst support for Wastewater Treatment. *Madridge J. Nanotechnol. Nanosci.* **2019**, *4*, 160–167. [[CrossRef](#)]
71. Pullukat, T.J.; Patterson, R.E. Porous Silica in Transition Metal Polymerization Catalysts. *Handb. Transit. Metal Polym. Catal.* **2018**, 31–55. [[CrossRef](#)]
72. Lee, J.S.; Yim, J.-H.; Jeon, J.-K.; Ko, Y.S. Polymerization of olefins with single-site catalyst anchored on amine-functionalized surface of SBA-15. *Catal. Today* **2012**, *185*, 175–182. [[CrossRef](#)]
73. McKittrick, M.W.; Jones, C.W. Toward Single-Site, Immobilized Molecular Catalysts: Site-Isolated Ti Ethylene Polymerization Catalysts Supported on Porous Silica. *J. Am. Chem. Soc.* **2004**, *126*, 3052–3053. [[CrossRef](#)]
74. Wilson, B.C. Silica-Supported Organic Catalysts for the Synthesis of Biodegradable Polymers. Ph.D. Dissertation, Georgia Institute of Technology, Atlanta, GA, USA, 2004; pp. 1–72.
75. Kusumastuti, H.; Trisunaryanti, W.; Falah, I.I.; Marsuki, M.F. Synthesis of mesoporous silica-alumina from lapindo mud as a support of ni and mo metals catalysts for hydrocracking of pyrolyzed α -cellulose. *Rasayan J. Chem.* **2018**, *11*, 522–530. [[CrossRef](#)]
76. Canhaci, S.J.; Perez, R.F.; Borges, L.E.; Fraga, M.A. Direct conversion of xylose to furfuryl alcohol on single organic–inorganic hybrid mesoporous silica-supported catalysts. *Appl. Catal. B Environ.* **2017**, *207*, 279–285. [[CrossRef](#)]
77. Masoud, N.; Delannoy, L.; Calers, C.; Gallet, J.-J.; Bournel, F.; De Jong, K.P.; Louis, C.; De Jongh, P.E. Silica-Supported Au–Ag Catalysts for the Selective Hydrogenation of Butadiene. *ChemCatChem* **2017**, *9*, 2418–2425. [[CrossRef](#)] [[PubMed](#)]
78. Großmann, D.; Klementiev, K.; Sinev, I.; Grünert, W. Surface Alloy or Metal-Cation Interaction—The State of Zn Promoting the Active Cu Sites in Methanol Synthesis Catalysts. *ChemCatChem* **2017**, *9*, 365–372. [[CrossRef](#)]
79. Gao, D.; Zhang, X.; Dai, X.; Qin, Y.; Duan, A.; Yu, Y.; Zhuo, H.; Zhao, H.; Zhang, P.; Jiang, Y.; et al. Morphology-selective synthesis of active and durable gold catalysts with high catalytic performance in the reduction of 4-nitrophenol. *Nano Res.* **2016**, *9*, 3099–3115. [[CrossRef](#)]
80. Qian, X.; Kuwahara, Y.; Mori, K.; Yamashita, H. Silver Nanoparticles Supported on CeO₂-SBA-15 by Microwave Irradiation Possess Metal-Support Interactions and Enhanced Catalytic Activity. *Chem. A Eur. J.* **2014**, *20*, 15746–15752. [[CrossRef](#)] [[PubMed](#)]
81. Mori, K.; Verma, P.; Hayashi, R.; Fukui, K.; Yamashita, H. Color-Controlled Ag Nanoparticles and Nanorods within Confined Mesopores: Microwave-Assisted Rapid Synthesis and Application in Plasmonic Catalysis under Visible-Light Irradiation. *Chem. A Eur. J.* **2015**, *21*, 11885–11893. [[CrossRef](#)] [[PubMed](#)]
82. Berro, Y.; Gueddida, S.; Bouzidi, Y.; Bellouard, C.; Bendeif, E.-E.; Gansmuller, A.; Celzard, A.; Fierro, V.; Ihiwakrim, D.; Ersen, O.; et al. Imprinting isolated single iron atoms onto mesoporous silica by templating with metallosurfactants. *J. Colloid Interface Sci.* **2020**, *573*, 193–203. [[CrossRef](#)] [[PubMed](#)]
83. Verma, P.; Kuwahara, Y.; Mori, K.; Yamashita, H. Enhancement of Ag-Based Plasmonic Photocatalysis in Hydrogen Production from Ammonia Borane by the Assistance of Single-Site Ti-Oxide Moieties within a Silica Framework. *Chem. A Eur. J.* **2017**, *23*, 3616–3622. [[CrossRef](#)]
84. Verma, P.; Kuwahara, Y.; Mori, K.; Yamashita, H. Synthesis and characterization of a Pd/Ag bimetallic nanocatalyst on SBA-15 mesoporous silica as a plasmonic catalyst. *J. Mater. Chem. A* **2015**, *3*, 18889–18897. [[CrossRef](#)]
85. Tasfy, S.F.H.; Shaharun, M.S.; Zabidi, N.A.M.; Subbarao, D. Effect of Mesoporous Silica Support on the Performance of Copper/Zinc Oxide Catalyst in Hydrogenation of CO₂ to Methanol. *Adv. Mater. Res.* **2015**, *1109*, 128–132. [[CrossRef](#)]
86. Tang, Y.; Gao, H.; Yang, M.; Wang, G.; Li, J.; Zhang, H.; Tao, Z. NiO promoted CuO–NiO/SBA-15 composites as highly active catalysts for epoxidation of olefins. *New J. Chem.* **2016**, *40*, 8543–8548. [[CrossRef](#)]
87. Jarupatrakorn, J.; Tilley, T.D.; Tantirungrotechai, J. Silica-Supported, Single-Site Titanium Catalysts for Olefin Epoxidation. A Molecular Precursor Strategy for Control of Catalyst Structure. *J. Am. Chem. Soc.* **2002**, *124*, 8380–8388. [[CrossRef](#)]
88. Cui, H.; Zhang, Y.; Qiu, Z.; Zhao, L.; Zhu, Y. Synthesis and characterization of cobalt-substituted SBA-15 and its high activity in epoxidation of styrene with molecular oxygen. *Appl. Catal. B Environ.* **2010**, *101*, 45–53. [[CrossRef](#)]

89. Avenier, P.; Taoufik, M.; Lesage, A.; Solans-Monfort, X.; Baudouin, A.; De Mallmann, A.; Veyre, L.; Basset, J.-M.; Eisenstein, O.; Emsley, L.; et al. Dinitrogen Dissociation on an Isolated Surface Tantalum Atom. *Science* **2007**, *317*, 1056–1060. [[CrossRef](#)] [[PubMed](#)]
90. Liu, S.; Zhang, L.; Zhang, L.; Zhang, H.; Ren, J. Function of well-established mesoporous layers of recrystallized ZSM-22 zeolites in the catalytic performance of n-alkane isomerization. *New J. Chem.* **2020**, *44*, 4744–4754. [[CrossRef](#)]
91. Zheng, M.; Ding, Y.; Cao, X.; Tian, T.; Lin, J. Homogeneous and heterogeneous photocatalytic water oxidation by polyoxometalates containing the most earth-abundant transition metal, iron. *Appl. Catal. B Environ.* **2018**, *237*, 1091–1100. [[CrossRef](#)]
92. Chang, F.; Jiao, M.; Xu, Q.; Deng, B.; Hu, X. Facile fabrication of mesoporous Fe-Ti-SBA15 silica with enhanced visible-light-driven simultaneous photocatalytic degradation and reduction reactions. *Appl. Surf. Sci.* **2018**, *435*, 708–717. [[CrossRef](#)]
93. Jeong, S.; Chung, K.-H.; Lee, H.; Park, H.; Jeon, K.-J.; Park, Y.-K.; Jung, S.-C. Enhancement of Hydrogen Evolution from Water Photocatalysis Using Liquid Phase Plasma on Metal Oxide-Loaded Photocatalysts. *ACS Sustain. Chem. Eng.* **2017**, *5*, 3659–3666. [[CrossRef](#)]
94. Kuwahara, Y.; Kaburagi, W.; Fujitani, T. Catalytic Conversion of Levulinic Acid and Its Esters to γ -Valerolactone over Silica-Supported Zirconia Catalysts. *Bull. Chem. Soc. Jpn.* **2014**, *87*, 1252–1254. [[CrossRef](#)]
95. Kuwahara, Y.; Kaburagi, W.; Osada, Y.; Fujitani, T.; Yamashita, H. Catalytic transfer hydrogenation of biomass-derived levulinic acid and its esters to γ -valerolactone over ZrO₂ catalyst supported on SBA-15 silica. *Catal. Today* **2017**, *281*, 418–428. [[CrossRef](#)]
96. Kou, J.; Sun, L.-B. Fabrication of Metal–Organic Frameworks inside Silica Nanopores with Significantly Enhanced Hydrostability and Catalytic Activity. *ACS Appl. Mater. Interfaces* **2018**, *10*, 12051–12059. [[CrossRef](#)]
97. Yang, Y.; Chang, J.W.; Rioux, R.M. Structural elucidation of supported Rh complexes derived from RhCl(PPh₃)₃ immobilized on surface-functionalized SBA-15 and their catalytic performance for C-heteroatom (S, O) bond formation. *J. Catal.* **2018**, *365*, 43–54. [[CrossRef](#)]
98. Wen, Z.; Duan, X.; Hu, M.; Cao, Y.; Ye, L.; Jiang, L.; Yuan, Y. Efficient low-temperature soot combustion by bimetallic Ag–Cu/SBA-15 catalysts. *J. Environ. Sci.* **2018**, *64*, 122–129. [[CrossRef](#)]
99. Shen, D.; Chen, L.; Yang, J.; Zhang, R.; Wei, Y.; Li, X.; Li, W.; Sun, Z.; Zhu, H.; Abdullah, A.M.; et al. Ultradispersed Palladium Nanoparticles in Three-Dimensional Dendritic Mesoporous Silica Nanospheres: Toward Active and Stable Heterogeneous Catalysts. *ACS Appl. Mater. Interfaces* **2015**, *7*, 17450–17459. [[CrossRef](#)]
100. Li, X.; Zheng, W.; Chen, B.; Wang, L.; He, G. Rapidly Constructing Multiple AuPt Nanoalloy Yolk@Shell Hollow Particles in Ordered Mesoporous Silica Microspheres for Highly Efficient Catalysis. *ACS Sustain. Chem. Eng.* **2016**, *4*, 2780–2788. [[CrossRef](#)]
101. Xie, W.; Wang, H. Grafting copolymerization of dual acidic ionic liquid on core-shell structured magnetic silica: A magnetically recyclable Brønsted acid catalyst for biodiesel production by one-pot transformation of low-quality oils. *Fuel* **2021**, *283*, 118893. [[CrossRef](#)]
102. Daneshjou, S.; Dabirmanesh, B.; Rahimi, F.; Jabbari, S.; Khajeh, K. Catalytic parameters and thermal stability of chondroitinase ABCI on red porous silicon nanoparticles. *J. Biotechnol.* **2020**, *324*, 83–90. [[CrossRef](#)] [[PubMed](#)]
103. Sun, Q.; Wang, N.; Xu, Q.; Yu, J. Nanopore-Supported Metal Nanocatalysts for Efficient Hydrogen Generation from Liquid-Phase Chemical Hydrogen Storage Materials. *Adv. Mater.* **2020**, *32*, e2001818. [[CrossRef](#)]
104. Martín, N.; Cirujano, F.G. Organic synthesis of high added value molecules with MOF catalysts. *Org. Biomol. Chem.* **2020**, *18*, 8058–8073. [[CrossRef](#)]
105. Haynes, T.; Bougnouch, O.; Dubois, V.; Hermans, S. Preparation of mesoporous silica nanocapsules with a high specific surface area by hard and soft dual templating approach: Application to biomass valorization catalysis. *Microporous Mesoporous Mater.* **2020**, *306*, 110400. [[CrossRef](#)]
106. Lee, J.; Dubbu, S.; Kumari, N.; Kumar, A.; Lim, J.; Kim, S.; Lee, I.S. Magnetothermia-Induced Catalytic Hollow Nanoreactor for Bioorthogonal Organic Synthesis in Living Cells. *Nano Lett.* **2020**, *20*, 6981–6988. [[CrossRef](#)]
107. Norouzi, N.; Das, M.K.; Richard, A.J.; Ibrahim, A.A.; El-Kaderi, H.M.; El-Shall, M.S. Heterogeneous catalysis by ultra-small bimetallic nanoparticles surpassing homogeneous catalysis for carbon–carbon bond forming reactions. *Nanoscale* **2020**, *12*, 19191–19202. [[CrossRef](#)]
108. Yang, G.; Yang, H.; Zhang, X.; Lqbal, K.; Feng, F.; Ma, J.; Qin, J.; Yuan, F.; Cai, Y.; Ma, J. Surfactant-free self-assembly to the synthesis of MoO₃ nanoparticles on mesoporous SiO₂ to form MoO₃/SiO₂ nanosphere networks with excellent oxidative desulfurization catalytic performance. *J. Hazard. Mater.* **2020**, *397*, 122654. [[CrossRef](#)]
109. Diaz, C.; Valenzuela, M.; Cifuentes-Vaca, O.; Segovia, M.; Laguna-Bercero, M. Iridium nanostructured metal oxide, its inclusion in silica matrix and their activity toward photodegradation of methylene blue. *Mater. Chem. Phys.* **2020**, *252*, 123276. [[CrossRef](#)]
110. Zhou, Z.; Li, X.; Wang, Y.; Luan, Y.; Li, X.; Du, X. Growth of Cu-BTC MOFs on dendrimer-like porous silica nanospheres for the catalytic aerobic epoxidation of olefins. *New J. Chem.* **2020**, *44*, 14350–14357. [[CrossRef](#)]
111. Heravi, M.M.; Heidari, B.; Zadsirjan, V.; Mohammadi, L. Applications of Cu(0) encapsulated nanocatalysts as superior catalytic systems in Cu-catalyzed organic transformations. *RSC Adv.* **2020**, *10*, 24893–24940. [[CrossRef](#)]
112. Isaeva, V.I.; Chernyshev, V.V.; Fomkin, A.A.; Shkolin, A.V.; Veselovsky, V.V.; Kapustin, G.I.; Sokolova, N.A.; Kustov, L.M. Preparation of novel hybrid catalyst with an hierarchical micro-/mesoporous structure by direct growth of the HKUST-1 nanoparticles inside mesoporous silica matrix (MMS). *Microporous Mesoporous Mater.* **2020**, *300*, 110136. [[CrossRef](#)]
113. Hemming, E.B.; Masters, A.F.; Maschmeyer, T. Exploring Opportunities for Platinum Nanoparticles Encapsulated in Porous Liquids as Hydrogenation Catalysts. *Chem. A Eur. J.* **2020**, *26*, 7059–7064. [[CrossRef](#)] [[PubMed](#)]

114. Jiang, Y.; Jiang, F.-Q.; Liao, X.; Lai, S.-L.; Wang, S.-B.; Xiong, X.-Q.; Zheng, J.; Liu, Y.-G. Customized three-dimensional porous catalyst for Knoevenagel reaction. *J. Porous Mater.* **2020**, *27*, 779–788. [[CrossRef](#)]
115. Kumari, E.; Görlich, S.; Poulsen, N.; Kröger, N. Genetically Programmed Regioselective Immobilization of Enzymes in Biosilica Microparticles. *Adv. Funct. Mater.* **2020**, *30*. [[CrossRef](#)]
116. Azizi, S.; Soleymani, J.; Shojaei, S.; Shadjou, N. Synthesize of folic acid functionalized dendritic fibrous nanosilica and its application as an efficient nanocatalyst for access to direct amidation of carboxylic acids with amines. *J. Nanostructures* **2020**, *10*, 671–681. [[CrossRef](#)]
117. Yan, P.; Zhang, X.; Wang, X.; Zhang, X. Controllable Preparation of Monodisperse Mesoporous Silica from Microspheres to Microcapsules and Catalytic Loading of Au Nanoparticles. *Langmuir* **2020**, *36*, 5271–5279. [[CrossRef](#)]
118. Casas-Luna, M.; Rodriguez, J.T.; Valdés-Martínez, O.U.; Obradović, N.; Slámečka, K.; Maca, K.; Kaiser, J.; Montufar, E.B.; Čelko, L. Robocasting of controlled porous CaSiO₃-SiO₂ structures: Architecture–Strength relationship and material catalytic behavior. *Ceram. Int.* **2020**, *46*, 8853–8861. [[CrossRef](#)]
119. Diaz, C.; Valenzuela, M.L.; Cifuentes-Vaca, O.; Segovia, M.; Laguna-Bercero, M.A. Incorporation of Nanostructured ReO₃ in Silica Matrix and Their Activity Toward Photodegradation of Blue Methylene. *J. Inorg. Organomet. Polym. Mater.* **2019**, *30*, 1726–1734. [[CrossRef](#)]
120. Li, Y.; Li, X.; Pillai, H.S.; Lattimer, J.; Adli, N.M.; Karakalos, S.G.; Chen, M.; Guo, L.; Xu, H.; Yang, J.; et al. Ternary PtIrNi Catalysts for Efficient Electrochemical Ammonia Oxidation. *ACS Catal.* **2020**, *10*, 3945–3957. [[CrossRef](#)]
121. Li, M.; Lv, J.; Wang, S.; Wang, J.; Lin, Y. Expanded mesoporous silica-encapsulated ultrasmall Pt nanoclusters as artificial enzymes for tracking hydrogen peroxide secretion from live cells. *Anal. Chim. Acta* **2020**, *1104*, 180–187. [[CrossRef](#)] [[PubMed](#)]
122. Toprakcioglu, Z.; Hakala, T.A.; Levin, A.; Becker, C.F.W.; Bernardes, G.J.L.; Knowles, T.P.J. Multi-scale microporous silica microcapsules from gas-in water-in oil emulsions. *Soft Matter* **2020**, *16*, 3082–3087. [[CrossRef](#)]
123. Elimbinzi, E.; Nyandoro, S.S.; Mubofu, E.B.; Manayil, J.C.; Lee, A.F.; Wilson, K. Valorization of rice husk silica waste: Organo-amine functionalized castor oil templated mesoporous silicas for biofuels synthesis. *Microporous Mesoporous Mater.* **2020**, *294*, 109868. [[CrossRef](#)]
124. Schulze, J.S.; Migenda, J.; Becker, M.; Schuler, S.M.M.; Wende, R.C.; Schreiner, P.R.; Smarsly, B.M. TEMPO-functionalized mesoporous silica particles as heterogeneous oxidation catalysts in flow. *J. Mater. Chem. A* **2020**, *8*, 4107–4117. [[CrossRef](#)]
125. Yang, J.; Fang, X.; Xu, Y.; Liu, X. Investigation of the deactivation behavior of Co catalysts in Fischer–Tropsch synthesis using encapsulated Co nanoparticles with controlled SiO₂ shell layer thickness. *Catal. Sci. Technol.* **2020**, *10*, 1182–1192. [[CrossRef](#)]
126. Purohit, G.; Rawat, D.S.; Reiser, O. Palladium Nanocatalysts Encapsulated on Porous Silica @ Magnetic Carbon-Coated Cobalt Nanoparticles for Sustainable Hydrogenation of Nitroarenes, Alkenes and Alkynes. *ChemCatChem* **2020**, *12*, 569–575. [[CrossRef](#)]
127. Tran, M.H.; Park, B.J.; Kim, B.H.; Yoon, H.H. Mesoporous silica template-derived nickel-cobalt bimetallic catalyst for urea oxidation and its application in a direct urea/H₂O₂ fuel cell. *Int. J. Hydrogen Energy* **2020**, *45*, 1784–1792. [[CrossRef](#)]
128. Kong, L.; Guo, Y.; Wang, X.; Zhang, X. Double-walled hierarchical porous silica nanotubes loaded Au nanoparticles in the interlayer as a high-performance catalyst. *Nanotechnology* **2019**, *31*, 015701. [[CrossRef](#)]
129. Mestre, R.; Cadefau, N.; Hortelão, A.C.; Grzelak, J.; Gich, M.; Roig, A.; Sánchez, S. Nanorods Based on Mesoporous Silica Containing Iron Oxide Nanoparticles as Catalytic Nanomotors: Study of Motion Dynamics. *ChemNanoMat* **2021**, *7*, 134–140. [[CrossRef](#)]
130. Chen, I.-H.; Lee, T.-Y.; Tseng, Y.-C.; Liou, J.-H.; Jan, J.-S. Biomineralization of mesoporous silica and metal nanoparticle/mesoporous silica nanohybrids by chemo-enzymatically prepared peptides. *Colloids Surfaces A Physicochem. Eng. Asp.* **2021**, *610*, 125753. [[CrossRef](#)]
131. Elahimehr, Z.; Nemati, F.; Elhampour, A. Synthesis of a magnetic-based yolk-shell nano-reactor: A new class of monofunctional catalyst by Cu₀-nanoparticles and its application as a highly effective and green catalyst for A₃ coupling reaction. *Arab. J. Chem.* **2020**, *13*, 3372–3382. [[CrossRef](#)]
132. Le Ferrand, H. Pressure-Less Processing of Ceramics with Deliberate Elongated Grain Orientation and Size. *Light Met.* **2020**, *2020*, 45–56.
133. Yang, Y.; Veser, G. Exploiting the impact of pore diffusion in core@shell nanocatalysts. *Catal. Today* **2020**, 2–9. [[CrossRef](#)]
134. Liu, N.; Zhao, S.; Yang, Z.-L.; Liu, B. Patchy Templated Synthesis of Macroporous Colloidal Hollow Spheres and Their Application as Catalytic Microreactors. *ACS Appl. Mater. Interfaces* **2019**, *11*, 47008–47014. [[CrossRef](#)]
135. Ribeiro, S.O.; Granadeiro, C.M.; Corvo, M.C.; Pires, J.; Campos-Martin, J.M.; De Castro, B.; Balula, S.S. Mesoporous Silica vs. Organosilica Composites to Desulfurize Diesel. *Front. Chem.* **2019**, *7*, 7. [[CrossRef](#)]
136. Kobayashi, J.; Kawamoto, K.; Kobayashi, N. Effect of porous silica on the removal of tar components generated from waste biomass during catalytic reforming. *Fuel Process. Technol.* **2019**, *194*, 106104. [[CrossRef](#)]
137. Wang, H.; Chen, Z.; Chen, D.; Yu, Q.; Yang, W.; Zhou, J.; Wu, S. Facile, template-free synthesis of macroporous SiO₂ as catalyst support towards highly enhanced catalytic performance for soot combustion. *Chem. Eng. J.* **2019**, *375*, 121958. [[CrossRef](#)]
138. Ayakar, S.R.; Yadav, G.D. Development of novel support for penicillin acylase and its application in 6-aminopenicillanic acid production. *Mol. Catal.* **2019**, *476*, 110484. [[CrossRef](#)]
139. Wu, X.-Q.; Shao, Z.-D.; Liu, Q.; Xie, Z.; Zhao, F.; Zheng, Y.-M. Flexible and porous TiO₂/SiO₂/carbon composite electrospun nanofiber mat with enhanced interfacial charge separation for photocatalytic degradation of organic pollutants in water. *J. Colloid Interface Sci.* **2019**, *553*, 156–166. [[CrossRef](#)]

140. Kinkead, B.; Malone, R.; Smith, G.; Pandey, A.; Trifkovic, M. Bicontinuous Intraphase Jammed Emulsion Gels: A New Soft Material Enabling Direct Isolation of Co-Continuous Hierarchical Porous Materials. *Chem. Mater.* **2019**, *31*, 7601–7607. [[CrossRef](#)]
141. Peng, L.; Li, Z.-W.; Zheng, R.-R.; Yu, H.; Dong, X.-T. Preparation and characterization of mesoporous g-C₃N₄/SiO₂ material with enhanced photocatalytic activity. *J. Mater. Res.* **2019**, *34*, 1785–1794. [[CrossRef](#)]
142. Xu, W.-M.; Chai, K.; Jiang, Y.-W.; Mao, J.; Wang, J.; Zhang, P.; Shi, Y. 2D Single Crystal WSe₂ and MoSe₂ Nanomeshes with Quantifiable High Exposure of Layer Edges from 3D Mesoporous Silica Template. *ACS Appl. Mater. Interfaces* **2019**, *11*, 17670–17677. [[CrossRef](#)]
143. Mahy, J.G.; Tasseroul, L.; Tromme, O.; Lavigne, B.; Lambert, S.D. Hydrodechlorination and complete degradation of chlorinated compounds with the coupled action of Pd/SiO₂ and Fe/SiO₂ catalysts: Towards industrial catalyst synthesis conditions. *J. Environ. Chem. Eng.* **2019**, *7*, 103014. [[CrossRef](#)]
144. Song, L.; Lin, Z.; Zhao, Y.; Hu, X.; Hong, Y.; Su, Y.; Wang, H.; Li, J. A CO₂-expanded gelation approach to prepare bimodal porous silica materials and their catalytic applications. *J. Supercrit. Fluids* **2019**, *144*, 91–97. [[CrossRef](#)]
145. Weinberger, C.; Heckel, T.; Schnippering, P.; Schmitz, M.; Guo, A.; Keil, W.; Marsmann, H.C.; Schmidt, C.; Tiemann, M.; Wilhelm, R. Straightforward Immobilization of Phosphonic Acids and Phosphoric Acid Esters on Mesoporous Silica and Their Application in an Asymmetric Aldol Reaction. *Nanomater.* **2019**, *9*, 249. [[CrossRef](#)]
146. Fathali, Z.; Rezaei, S.; Faramarzi, M.A.; Habibi-Rezaei, M. Catalytic phenol removal using entrapped cross-linked laccase aggregates. *Int. J. Biol. Macromol.* **2019**, *122*, 359–366. [[CrossRef](#)]
147. Wang, Y.; Chen, Z.; Fang, R.; Li, Y.; Chen, Z. Hollow-Co₃O₄@Co₃O₄@SiO₂ Multi-Yolk-Double-Shell Nanoreactors for Highly Efficient CO Oxidation. *ChemCatChem* **2019**, *11*, 772–779. [[CrossRef](#)]
148. Bolshakov, A.; Van Diepen, M.; Van Hoof, A.J.F.; Hidalgo, D.E.R.; Kosinov, N.; Hensen, E.J.M. Hierarchically Porous (Alumino)Silicates Prepared by an Imidazole-Based Surfactant and Their Application in Acid-Catalyzed Reactions. *ACS Appl. Mater. Interfaces* **2019**, *11*, 40151–40162. [[CrossRef](#)] [[PubMed](#)]
149. Gößl, D.; Singer, H.; Chiu, H.-Y.; Schmidt, A.; Lichtnecker, M.; Engelke, H.; Bein, T. Highly active enzymes immobilized in large pore colloidal mesoporous silica nanoparticles. *New J. Chem.* **2018**, *43*, 1671–1680. [[CrossRef](#)]